Check for updates

Received: 20 January 2021 | Revised: 18 February 2021 | Accepted: 21 March 2021

DOI: 10.1111/pace.14228

PACE WILEY

ELECTROPHYSIOLOGY

A multi-center experience of ablation index for evaluating lesion delivery in typical atrial flutter

Edd Maclean MD[1,2] | Ron Simon MD[1] | Richard Ang MD, PhD[1] | Gurpreet Dhillon MD[1] | Syed Ahsan MD[1] | Fakhar Khan MD[1] | Mark Earley MD[1] | Pier D. Lambiase MD, PhD[1] | James Rosengarten MD[1] | Anthony W. Chow MD[1] | Mehul Dhinoja MD[1] | Rui Providencia MD, PhD[1] | Vias Markides MD[1] | Tom Wong MD[3] | Ross J. Hunter MD PhD[1,2] | Jonathan M. Behar MD, PhD[1,2,3]

[1] Department of Cardiac Electrophysiology, St Bartholomew's Hospital, W Smithfield, London, UK

[2] William Harvey Research Institute, Queen Mary University of London, London, UK

[3] Department of Cardiac Electrophysiology, Royal Brompton Hospital, London, UK

Correspondence
Jonathan M. Behar MD, PhD, Department of Cardiac Electrophysiology, Royal Brompton Hospital, Sydney Street, London SW3 6NP, UK.
Email: j.behar@rbht.nhs.uk

Abstract

Background: Anatomical studies demonstrate significant variation in cavotricuspid isthmus (CTI) architecture.

Methods: Thirty-eight patients underwent CTI ablation at two tertiary centers. Operators delivered 682 lesions with a target ablation index (AI) of 600 Wgs. Ablation parameters were recorded every 10–20 ms. Post hoc, Visitags were trisected according to CTI position: inferior vena cava (IVC), middle (Mid), or ventricular (V) lesions.

Results: There were no complications. 92.1% of patients (n = 35) remained in sinus rhythm after 14.6 ± 3.4 months. For the whole CTI, peak AI correlated with mean impedance drop (ID) ($R^2 = 0.89$, $p < .0001$). However, analysis by anatomical site demonstrated a non-linear relationship Mid CTI ($R^2 = 0.15$, $p = .21$). Accordingly, while mean AI was highest Mid CTI (IVC: 473.1 ± 122.1 Wgs, Mid: 539.6 ± 103.5 Wgs, V: 486.2 ± 111.8 Wgs, ANOVA $p < .0001$), mean ID was lower (IVC: 10.7 ± 7.5Ω, Mid: 9.0 ± 6.5Ω, V: 10.9 ± 7.3Ω, $p = .011$), and rate of ID was slower (IVC: 0.37 ± 0.05 Ω/s, Mid: 0.18 ± 0.08 Ω/s, V: 0.29 ± 0.06 Ω/s, $p < .0001$). Mean contact force was similar at all sites; however, temporal fluctuations in contact force (IVC: 19.3 ± 12.0 mg/s, Mid: 188.8 ± 92.1 mg/s, V: 102.8 ± 32.3 mg/s, $p < .0001$) and catheter angle (IVC: 0.42°/s, Mid: 3.4°/s, V: 0.28°/s, $p < .0001$) were greatest Mid CTI. Use of a long sheath attenuated these fluctuations and improved energy delivery.

Conclusions: Ablation characteristics vary across the CTI. At the Mid CTI, higher AI values do not necessarily deliver more effective ablation; this may reflect localized fluctuations in catheter angle and contact force.

KEYWORDS
ablation index, atrial flutter, catheter ablation, cavo-tricuspid isthmus, force sensing

Abbreviations: AF, atrial fibrillation; AI, Ablation Index; CTI, cavotricuspid isthmus; ID, impedance drop; LVEF, left ventricular ejection fraction; PVI, pulmonary vein isolation; Wgs, Watts/grams/second; Ω, Ohms.

This is an open access article under the terms of the Creative Commons Attribution-NonCommercial License, which permits use, distribution and reproduction in any medium, provided the original work is properly cited and is not used for commercial purposes.
© 2021 The Authors. *Pacing and Clinical Electrophysiology* published by Wiley Periodicals LLC.

1 | INTRODUCTION

The advent of contact force-sensing catheters has delivered important data on ablation lesion size, safety and efficacy, and their application is well-described during pulmonary vein isolation (PVI) for atrial fibrillation (AF).[1–3] Using a weighted formula, catheter contact force (g) can be combined with the duration (s) and power (W) of a radiofrequency application to calculate Ablation Index (AI). Expressed as a continuous value in Wgs, AI has been shown to predict lesion diameter and depth during AF ablation,[4] and left atrial procedures guided by site-specific AI targets have demonstrated more enduring PVI and a comparable safety profile versus conventional ablation techniques.[5–8] AI infers the energy delivered by the ablation catheter; this differs from impedance drop (ID) which describes local impedance changes at the blood-tissue interface and infers tissue receipt of injury. While AI is known to correlate with ID, the strength of this relationship attenuates with procedural variables such as catheter angle of incidence and irrigation techniques; as such, there may be important limitations when relying on AI alone to guide lesion delivery.[9,10]

Radiofrequency ablation of cavo-tricuspid isthmus (CTI) dependent ("typical") atrial flutter achieves acute success (i.e., bidirectional block) in over 90% of cases, and carries a class IA recommendation as a treatment strategy in the ESC's 2019 Supraventricular Tachycardia (SVT) guidelines.[11,12] Despite this, a significant proportion of CTI ablations can prove technically challenging, and hence novel predictors of acute and long-term efficacy remain desirable. Autopsy studies have demonstrated marked heterogeneity in CTI architecture; Klimek-Piotrowska et al. dissected 140 human hearts and found that, when compared to the anterior or posterior margins, the middle (Mid) CTI frequently harbors distinct morphological variations such as trabeculae (62.1%) or recesses (25%).[13] Peri-ablation imaging data has also shown that structural anomalies—such as the presence of pouches, angular crypts or tricuspid regurgitation—result in prolonged procedure times and poorer outcomes.[14,15] Accordingly, data from contact-force sensing catheters suggests that site-specific inconsistencies in isthmus tissue contact may be responsible for procedural failure.[16] The prevalence of complex CTI anatomy has led some authors to suggest that pre-procedural imaging, such as cardiac MRI or right atrial angiography, would promote more patient-specific ablation strategies and hence improve outcomes.[15,17]

1.1 | Hypothesis

We hypothesized that AI may provide important insights into lesion delivery across the CTI during ablation of typical atrial flutter. Using established 3D electro-anatomical mapping systems and ablation catheters, examining local variations in ablation lesion characteristics may elucidate the mechanisms which impede enduring bidirectional block or contribute to complications. An appreciation of these relationships may promote a more prescriptive approach to CTI ablation without the use of additional resources such as peri- or intraprocedural imaging techniques.

2 | METHODS

2.1 | Ethics

This project was registered with the local clinical effectiveness unit. Consenting patients underwent procedures which were clinically indicated, without randomization or allocation, and which made use well-established mapping and ablation techniques. As such, the work was consistent with Clinical Service Development in line with the UK's Health Research Authority recommendations, and no specific additional ethical approval was required.

2.2 | Participants

Patients were referred for ablation if they had ECG evidence of symptomatic CTI-dependent atrial flutter. Individuals with co-existent atrial fibrillation or previous atrial ablation were excluded. Standalone radiofrequency CTI ablation took place at two tertiary Cardiothoracic hospitals in the UK from 2019 to 2020.

2.3 | Procedure

Procedures were performed on uninterrupted oral anticoagulation, either under general anesthetic or with conscious intravenous sedation. Ultrasound-guided femoral venepuncture was performed following local anesthetic administration, and a quadripolar or decapolar catheter was positioned in the coronary sinus. A contact-force sensing ablation catheter (Thermocool SmartTouch, Biosense Webster, Diamond Bar, California, USA) was passed to the right atrium. Electro-anatomical mapping was performed using CARTO software (v3, Biosense Webster). For patients presenting in atrial flutter, entrainment discerned CTI dependence, whereas patients in sinus rhythm underwent empirical CTI ablation during pacing of the proximal coronary sinus at 600 ms. Point-by-point ablation was delivered from the ventricular margin of the CTI progressing towards the inferior vena cava (IVC), maintaining a 6 o'clock alignment in the left anterior oblique projection as per standard clinical protocol. The use of additional sheaths to guide ablation was at the operators' discretion. Ablation VisiTag settings were pre-specified to accept 5 mm of catheter drift, and force-over-time (FOT) constraints of 5 s, 25% in conjunction with 3 g minimum force. Operators were advised to deliver ablation lesions with a peak AI of 600 Wgs at 45–50W. These recommendations were based on a retrospective analysis performed at our institution which demonstrated safe and effective CTI ablation with clusters of lesions in this range of AI.[18] In the event of visual macro-displacement, locations were discarded. Saline irrigation flow rate was 2 mL/min during mapping and 17–30 mL/min during ablation. Impedance was measured between the catheter tip and a ground patch on the patient's right thigh. If bidirectional CTI block was achieved, this was reassessed after 15 min' observation; consolidative ablation lesions were delivered as required. In the absence of complications, patients were

discharged the same day if the procedure was performed under sedation, or the following day if performed under general anesthetic.

2.4 | Data extraction

Post hoc, VisiTags were anatomically trisected according to their position on the CTI: IVC end (IVC), middle CTI (Mid), or ventricular end (V). Lesion characteristics were subsequently extracted and aligned with time stamps to allow assessment of temporal changes, including contact force (every 50 ms), impedance, ID and AI (every 10–20 ms), catheter angle in the axial and lateral planes (every 10–20 ms), and power (every 100 ms). It has been demonstrated that precipitous rises in impedance are associated with thrombus and steam formation, and a variety of methods for assessing change in impedance during catheter ablation have been published previously, including total ID, overall median ID, or median ID after 10 s of ablation.[2,9,19] During our data cleaning, very rare transient spikes and troughs (lasting <50 ms) in impedance–and consequently the running calculations of ID–were noted. The examination of other contemporaneous lesion characteristics (e.g., contact force) suggested that these data points were real, and as their ramifications on ablation safety were potentially significant, they were included in further analyses. However, these outlying values rendered the measurement of total ID less reliable, and so a mean ID was instead calculated from all the values recorded throughout the duration of each radiofrequency application. The mean ID was assigned as a surrogate marker of ablation efficacy. Total energy delivery was assessed in terms of peak AI; this was defined as the maximum recorded AI (Wgs) measured during each lesion; for all VisiTags, this corresponded to the final recorded value.

2.5 | Follow-up

All patients underwent clinical review and 12 lead ECG at 3 and 12 months post procedure. Additional interim 24 h holter analysis was performed in three patients who reported a resumption of symptoms, and four patients presented data from wearable devices at follow-up review. Anticoagulation was continued according to CHA_2DS_2-VASc score, and anti-arrhythmic drugs were adjusted according to patient preference and physicians' discretion.

2.6 | Statistical analysis

Data were analyzed in R (x64, v. 3.5.2.) and XLSTAT (Addinsoft, v. 2020.1). Categorical group parameters were compared using Chi square tests. The Shapiro-Wilk test identified whether or not data were normally distributed. Subsequently, continuous data were compared with two-tailed *T* tests or analysis of variance (ANOVA) with post-hoc Tukey HSD testing for normally distributed data, or with the Mann-Whitney *U* or Kruskal-Wallis test for non-normally distributed data. Correlation was assessed using Pearson's coefficient for normally distributed data or the Spearman rank correlation if non-normally distributed. Data are presented as mean ± SD or median (interquartile range). The level of significance was set at $p < .05$.

TABLE 1 Clinical characteristics and baseline ablation data

Clinical characteristics	
Age (years)	71 (15.5)
Male	89.5% (n = 34)
Duration of atrial flutter (months)	8.5 (8)
Hypertension	23.7% (n = 9)
Diabetes	15.8% (n = 6)
Smoking history	13.2% (n = 5)
Ischemic heart disease (previous PCI or CABG)	10.5% (n = 4)
Congenital heart disease	2.6% (n = 1; coarctation of the aorta)
Beta blocker	86.8% (n = 33)
Class III anti-arrhythmic drug	15.8% (n = 6)
Anticoagulated with DOAC (remainder warfarin)	92.1% (n = 35)
LV ejection fraction (%)	55 (10)
Baseline ablation data	
General anesthetic	23.7% (n = 9)
Procedure started in sinus rhythm	23.7% (n = 9)
Long sheath used	36.8% (n = 14)
Procedure time (min)	61.4 ± 37.1
Fluoroscopy time (min)	2.7 ± 4.7
Dose area product (cGy/cm^2)	78.6 ± 254

Parameters listed for 38 patients undergoing CTI ablation as % (n), mean ± SD, or median (IQR).

3 | RESULTS

Thirty-eight individuals were included in this study; clinical characteristics and baseline ablation data are shown in Table 1. Fourteen cases made use of additional long sheaths (11 Swartz SR0, Abbott/St Jude Medical; two Agilis, Abbott/St Jude Medical, one Vizigo, Biosense Webster) to assist ablation. Acute success (bidirectional block) was achieved in all 38 cases (100%); however, failure to achieve bidirectional block first pass was seen in five patients (13.2%). In these cases, bidirectional block was achieved following consolidative ablation at the Mid CTI in four patients, and at the IVC end in one patient. There were no complications, and no steam pops were recorded. After a mean follow-up of 14.6 ± 3.4 months, 92.1% (n = 35) of patients were in sinus rhythm.

Ablation lesion characteristics are summarized in Table 2. Across all procedures, a total of 682 ablation lesions were delivered (IVC: 206, Mid CTI: 242, V: 234) and 6,187,716 data points extracted. The number of ablation lesions per procedure ranged from 5 to 44. For the

TABLE 2 Ablation lesion characteristics across the CTI

Parameter	Whole CTI	IVC	Middle	Ventricular	*p*
Peak AI (Wgs)	499.6 ± 91.6	473.1 ± 122.1	539.6 ± 103.5	486.2 ± 111.8	*Mid vs. IVC or V* **$p < .0001$** *IVC vs. V* $p = .63$
Power (W)	45.1 ± 4.3	45.0 ± 4.3	44.8 ± 4.6	45.8 ± 4.1	*All* $p > 0.1$
Lesion duration (s)	23.7 ± 13.2	21.9 ± 14.5	28.9 ± 12.4	22.0 ± 15.2	*Mid vs. IVC or V* **$p < .0001$** *IVC vs. V* $p = .98$
Contact force (g)	10.5 ± 7.3	10.4 ± 7.2	10.6 ± 7.6	10.3 ± 7.3	*All* $p > .1$
Impedance drop (Ohms)	9.7 ± 5.7	10.7 ± 7.5	9.0 ± 6.5	10.9 ± 7.3	*Mid vs. IVC* $p = .011$, *Mid vs. V* $p = .005$ *IVC vs. V* $p = .76$
Rate of impedance drop (Ohms/s)	0.28 ± 0.03	0.37 ± 0.05	0.18 ± 0.08	0.29 ± 0.06	*All* $p < .0001$
Temperature (°C)	37.4 ± 4.6	38.1 ± 4.4	36.2 ± 5.4	37.8 ± 4.0	*Mid vs. IVC or V* **$p < .0001$** *IVC vs. V* $p = .52$

Lesion components listed for the CTI as a whole and stratified according to anatomical site. Significant *p* values (< .05) are highlighted in bold.

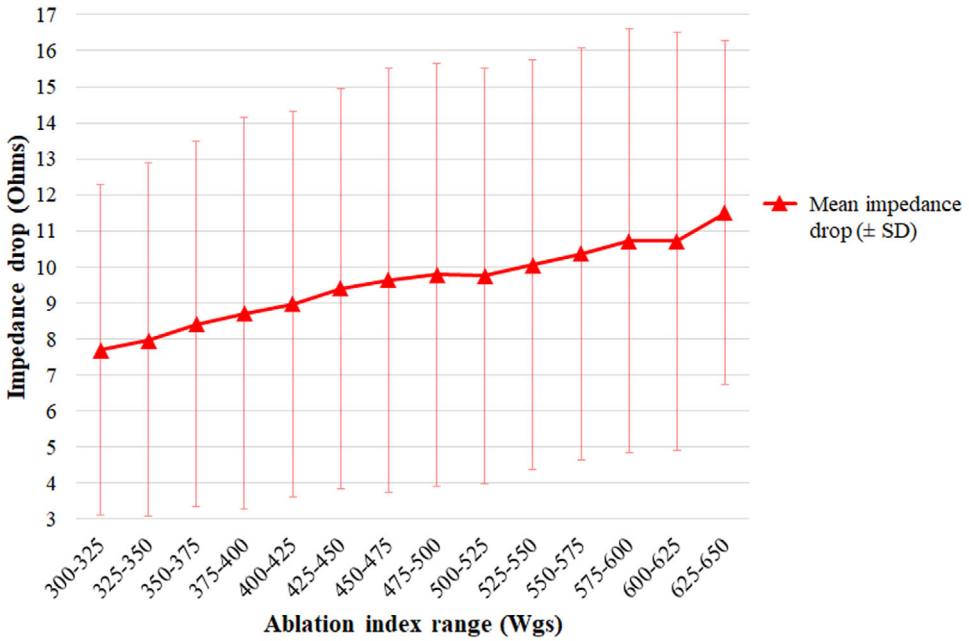

FIGURE 1 Relationship between peak ablation index (Wgs) and mean impedance drop (Ohms; mean ± SD) for all CTI lesions. Pearson's $R^2 = 0.89$, $p < .0001$ [Color figure can be viewed at wileyonlinelibrary.com]

whole CTI, there was a strong correlation between peak AI and mean ID (Figure 1–$R^2 = 0.89$, $p < .0001$). However, analysis by anatomical site demonstrated significant variation in this relationship (Figure 2). While AI and ID maintained a strong linear association at the V and IVC margins, at the Mid CTI linearity was less apparent with a qualitative plateau in ID noted beyond AI of 500 Wgs (Figure 2–$R^2 = 0.15$, $p = .21$). Longer lesion duration was also required Mid CTI to achieve the target AI (Table 2). In addition, while mean peak AI was highest Mid CTI, mean ID was lower, and rate of ID was slower Mid CTI (Table 2). Mean contact force and power were similar at all sites; however, mean temperature was lowest Mid CTI (Table 2).

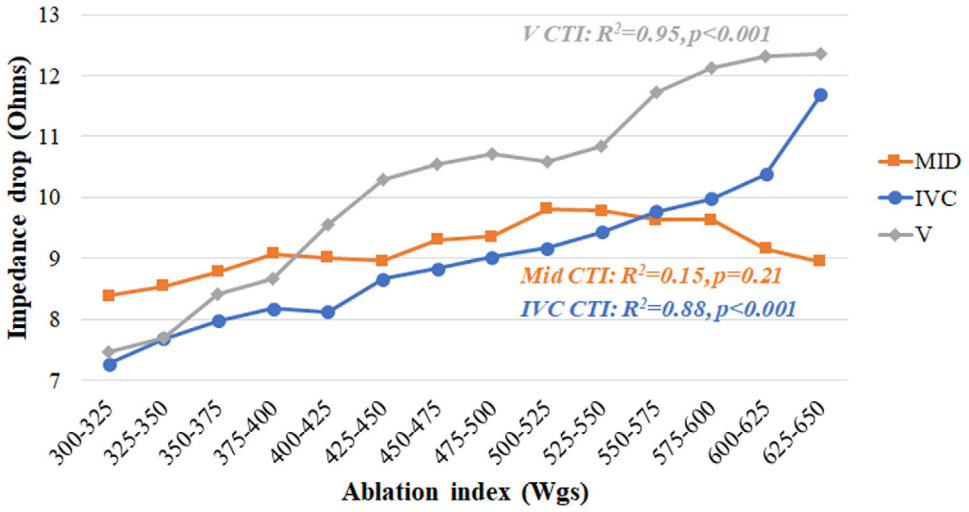

FIGURE 2 Relationship between peak ablation index (Wgs) and mean impedance drop (Ohms) per lesion according to CTI anatomical site (V CTI $R^2 = 0.95$, $p < .0001$, Mid CTI $R^2 = 0.15$, $p = .21$, IVC CTI $R^2 = 0.88$, $p < .0001$) [Color figure can be viewed at wileyonlinelibrary.com]

TABLE 3 Variation in contact force across the CTI

Parameter	Whole CTI	IVC	Middle	Ventricular	*p*
Temporal fluctuation in contact force (mg/s)–no sheath used	103.5 ± 93.8	19.3 ± 12.0	188.8 ± 92.1	102.8 ± 32.3	*All < .0001*
Temporal fluctuation in contact force (mg/s)–long sheath used	31.0 ± 18.3	16.1 ± 7.3	36.5 ± 17.2	40.8 ± 17.7	*IVC vs. Mid or IVC vs. V < .0001, Mid vs. V p = .085*
p	*<.0001*	*.025*	*<.0001*	*<.0001*	

Significant *p* values (< .05) are highlighted in bold.

Given that these findings suggested that comparable energy applications (according to AI) produced inconsistent degrees of tissue injury (by ID) at different CTI sites despite similar mean contact force and power, further analysis was performed to examine the catheter-tissue interface.

Temporal fluctuation in contact force was determined by examining the change in recorded catheter force (g) every 50 ms. A mean value for each lesion (total fluctuation divided by lesion duration) was calculated and expressed in mg/s. Variation was greatest Mid CTI (Table 3) and was amplified in lesions with higher peak AI values. However, use of a long sheath significantly reduced temporal fluctuations in contact force throughout the CTI (Table 3, Figure 3).

Fluctuation in catheter angle of incidence was assessed in both the axial and lateral planes. For each lesion, change in catheter angle was recorded every 10–20 ms and the average value determined in degrees/s. Variations in catheter tip angle were most marked at the Mid CTI (*Lateral plane*–IVC: 0.82 ± 0.4 degrees/s, Mid: 2.83 ± 1.1 degrees/s, V: 1.0 ± 0.6 degrees/s, $p < .0001$; *Axial plane*–IVC: 0.42 ± 0.2 degrees/s, Mid: 3.4 ± 1.3 degrees/s, V: 0.28 ± 0.2 degrees/s, $p < .0001$) but again diminished with the use of a long sheath (Figure 4). As these findings inferred that the use of a long sheath attenuated the catheter tip instability seen at the Mid CTI, the relationship between AI and ID was re-examined according to sheath use (Table 4). Despite a trend towards lower peak AI, use of a long sheath at the Mid CTI was associated with a greater and more rapid drop in impedance.

4 | DISCUSSION

Our study made use of AI to examine ablation lesion characteristics in the treatment of typical atrial flutter. We found that using a target AI of 600 Wgs across the CTI was safe, but there were significant inconsistencies in energy delivery according to anatomical site, with particularly notable variance seen in the Mid CTI.

While mean contact force and power were similar across all CTI sites, higher peak AI values were seen Mid CTI, which appears to be mediated through compensatory increases in lesion duration. However, at this site, increased peak AI values did not necessarily correlate with greater ID, and both the rate of ID and the mean lesion temperature were significantly lower at this site despite similar catheter

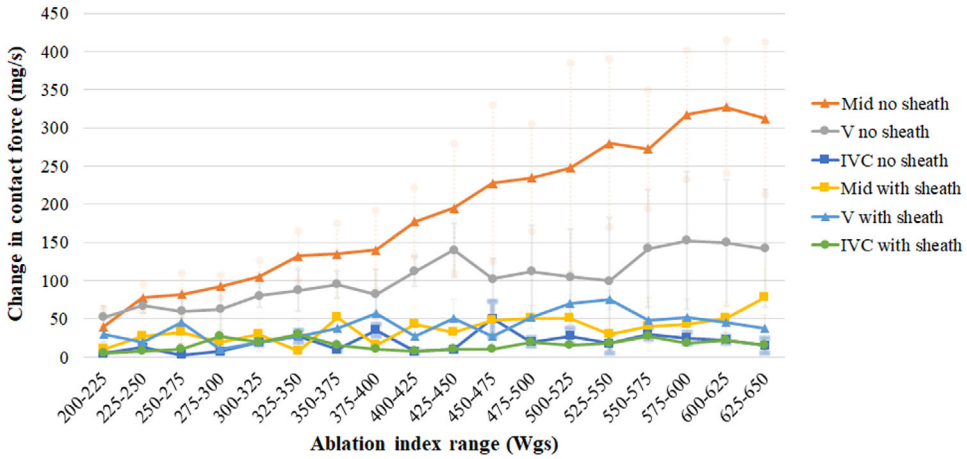

FIGURE 3 Average temporal fluctuation in contact force (mg/s) per ablation lesion according to peak ablation index, stratified according to CTI anatomical site and the use of a long sheath [Color figure can be viewed at wileyonlinelibrary.com]

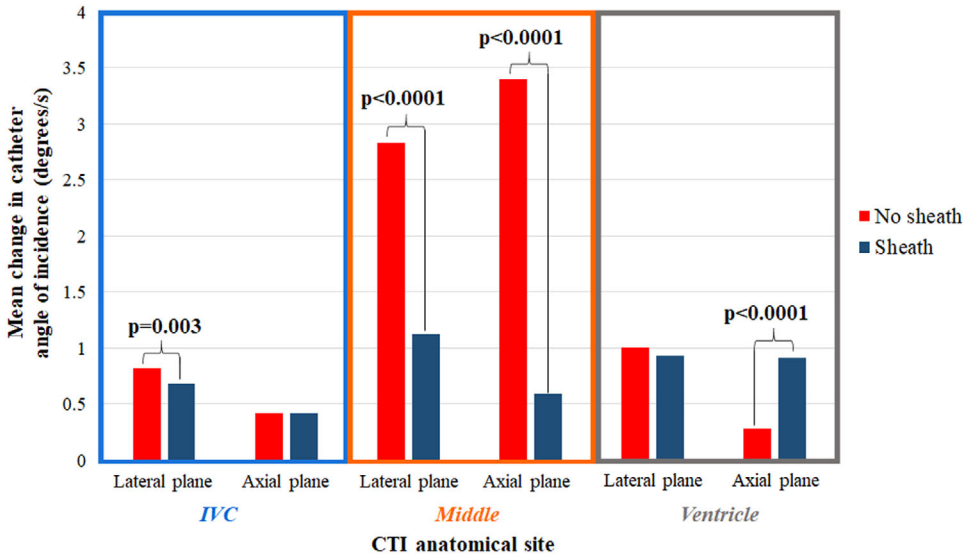

FIGURE 4 Average temporal fluctuation in catheter angle of incidence (degrees/s) in the lateral and axial planes for each ablation lesion, stratified according to CTI anatomical site and the use of a long sheath. Significant *p* values highlighted; other relationships non-significant [Color figure can be viewed at wileyonlinelibrary.com]

TABLE 4 Ablation lesion characteristics at the Mid CTI according to sheath use

Parameter	Middle CTI: no sheath (n = 152)	Middle CTI: long sheath used (n = 90)	*p*
Peak AI (Wgs)	549.2 ± 103.5	523.4 ± 99.6	*.058*
Power (W)	45.0 ± 4.9	44.5 ± 4.1	*.44*
Lesion duration (s)	30.9 ± 13.2	25.5 ± 14.3	*.0032*
Contact force (g)	10.2 ± 6.6	11.2 ± 8.1	*.29*
Impedance drop (Ohms)	8.2 ± 7.4	10.4 ± 7.1	*.024*
Rate of impedance drop (Ohms/s)	0.15 ± 0.12	0.23 ± 0.16	*<.0001*

Significant *p* values (< .05) are highlighted in bold.

tip power, mean contact force and irrigation techniques, suggestive of inferior lesion efficacy.

We propose this occurs because of significant temporal fluctuations in contact force and catheter tip angle which are most exaggerated at the Mid CTI (Figures 3 and 4). It is accepted that changes in catheter angle of incidence affect lesion size,[10] and that consistent tissue contact produces larger lesions than intermittent contact.[20] The fluctuations seen in our study are likely to indicate catheter tip instability encountered due to established anatomical anomalies Mid CTI, and these became more pronounced at higher AI values (Figure 3).[13] This may reflect the challenges of maintaining consistent contact during more prolonged ablation at the Mid CTI, whereby catheter flexion over the Eustachian ridge may exert a fulcrum effect on the distal tip, destabilizing lesion delivery. Consequently, while the relationship between AI and ID is mostly linear (Figures 1 and 2)–and hence peak AI is a reasonable surrogate for lesion efficacy in atrial flutter–we suggest that operators should exercise caution at the Mid CTI, where higher peak AI values do not necessarily equate to more effective ablation. Importantly, the use of a long sheath appears to confer additional stability to the catheter tip and overcome the majority of inconsistencies in force and angle, although a significant increase in axial plane fluctuation was noted at the ventricular margin (Figure 4). This finding may represent catheter and sheath overreach at the point of the valve annulus into the ventricular inflow tract; a long sheath remained effective in stabilizing contact force at this site.

The optimal AI for safe and effective CTI ablation is not well established; our target AI of 600 Wgs was based on retrospective analysis performed at our center,[18] and is in excess of that which is generally recommended for left atrial procedures. Importantly, we did not record any acute or long-term complications with our protocol for CTI ablation. Our mechanistic study was not designed to assess long-term procedural efficacy; however, it is encouraging that 92.1% of patients were in sinus rhythm after 12 months' follow-up. Longer term clinical review is in progress.

To our knowledge, we are the second group to analyze AI in the ablation of atrial flutter. Zhang et al. compared AI-guided ablation versus contact-force guided ablation of the CTI, and found higher rates of first-pass conduction block in their AI-guided group.[21] These authors delivered ablation with AI targets of 500 Wgs to the anterior two thirds of the CTI and 400 Wgs to the posterior third; these target values were derived from studies of PVI and adjusted according to accepted variations in CTI thickness. They found that acute reconnection of the CTI was more common at the ventricular aspect of the CTI with AI values of <450 Wgs. In contrast to our study, the authors' protocol delivered higher AI values at the anterior segments and found that this was associated with a relatively larger drop in impedance. Temporal changes in contact force or catheter angle, and the correlation of ID with different peak AI values, were not examined. Our study is the first to make use of precise AI-associated lesion delivery characteristics to define the heterogeneity encountered when ablating the CTI.

While our findings may have been more sharply delineated with the addition of peri- or -intraprocedural imaging studies, in clinical practice outcomes for CTI ablation without these techniques are already reasonable.[11] Accordingly, our aim was to explore a novel utility of an existing technology as a vehicle for incremental improvements in procedural success and safety, which could be adopted clinically without considerable additional resources.

Our study has important limitations. While our patient sample is multicenter, patient numbers are small; the number of extracted lesion data points were sufficient to permit key analyses; however, pertinent comparisons of additional potential confounders—for example., catheter curve, patient co-morbidities, or the use of general anesthetic or of class III anti-arrhythmic drugs—could not be performed. Likewise, failure to achieve bidirectional block first pass occurred most frequently due to incomplete ablation at the Mid CTI; this finding is in line with our study's principal conclusions, but the incidence of first pass failure was insufficient to allow more informative modeling. AI itself is validated only for ablation catheters made by Biosense Webster; our results may not be generalizable to equipment from other manufacturers. Likewise, our operators did not use surround flow (STSF) catheters, which are known to have different biophysical efficacy than their ST equivalent and hence our findings cannot be extrapolated to this technology.[9] We used a measure of ID as marker of ablation efficacy; this is a widely accepted surrogate in the literature; however, histological analysis is the gold standard for the assessment of lesion quality and this was not available in our study.

5 | CONCLUSIONS

In the ablation of CTI-dependent atrial flutter, the use of AI appears safe when delivering lesions up to 600 Wgs. While AI is generally a reliable marker of ablation efficacy by ID, we suggest that operators exercise caution when interpreting AI values at the Mid CTI, where anatomical anomalies may introduce catheter instability and hence impede energy delivery. Higher AI values are required Mid CTI to deliver lesions comparable to the CTI margins, and this phenomenon seems to be mediated by temporal fluctuations in contact force and catheter angle. It appears that the use of a long sheath may mitigate these fluctuations and restore a more linear relationship between AI and ID. In the absence of a long sheath, an ablation strategy which prescribes higher AI targets to the Mid CTI may improve acute lesion efficacy and hence long-term outcomes; however, this requires prospective validation.

ACKNOWLEDGMENTS

Jonathan M. Behar received an educational grant from Biosense Webster in relation to this work. Ross J. Hunter has received educational grants from Medtronic and from Biosense Webster in relation to a different study, Vias Markides has received speaker fees and travel support from Biosense Webster, Tom Wong has received research funding support from St. Jude Medical/Abbott, Anthony W. Chow has received educational grants from Boston and speaker fees from St. Jude Medical/Abbott, Pier D. Lambiase is supported by the NIHR UCLH/UCL and Barts Biomedical Research Centers, and has received speaker fees,

research and educational grants from Boston Scientific and research grants from St. Jude Medical/Abbott and Medtronic. The other authors have no relevant disclosures.

CONFLICTS OF INTEREST

All authors take responsibility for all aspects of the reliability and freedom from bias of the data presented and their discussed interpretation.

DATA AVAILABILITY STATEMENT

Upon reasonable request.

ORCID

Edd Maclean MD https://orcid.org/0000-0001-6177-2221

REFERENCES

1. Thiagalingam A, D'Avila A, Foley L, et al. Importance of catheter contact force during irrigated radiofrequency ablation: evaluation in a porcine ex vivo model using a force-sensing catheter. *J Cardiovasc Electrophysiol*. 2010;21:806-811.
2. Yokoyama K, Nakagawa H, Shah DC, et al. Contact force sensor incorporated in irrigated radiofrequency ablation catheter predicts lesion size and incidence of steam pop and thrombus. *CircArrhythmia Electrophysiol*. 2008;1:354-362.
3. Reddy V, Shah D, Kautzner J, et al. The relationship between contact force and clinical outcome during radiofrequency catheter ablation of atrial fibrillation in the TOCCATA study. *Heart Rhythm*. 2012;9:1789-1795.
4. Nakagawa H, Ikeda A, Govari A, Papaioannou T, Constantine G, Bar-Tal M. Prospective study to test the ability to create RF lesions at predicted depths of 3, 5, 7 and 9 mm using a new formula incorporating contact force, radiofrequency power and application time (force-power-time index) in the beating canine heart. *Heart Rhythm*. 2013;10:S481.
5. Hussein A, Das M, Chaturvedi V, et al. Prospective use of ablation index targets improves clinical outcomes following ablation for atrial fibrillation. *J Cardiovasc Electrophysiol*. 2017;28:1037-1047.
6. Pranata R, Vania R, Huang I. Ablation-index guided versus conventional contact-force guided ablation in pulmonary vein isolation–Systematic review and meta-analysis. *Indian Pacing Electrophysiol J*. 2019;19:155-160.
7. Santoro F, Metzner A, Brunetti ND, et al. Left atrial anterior line ablation using ablation index and inter-lesion distance measurement. *Clin Res Cardiol*. 2019;108:1009-1016.
8. Phlips T, Taghji P, El Haddad M, et al. Improving procedural and one-year outcome after contact force-guided pulmonary vein isolation: the role of interlesion distance, ablation index, and contact force variability in the 'CLOSE'-protocol. *Europace*. 2018;1:f419-f427.
9. Ullah W, Hunter RJ, Finlay MC, et al. Ablation index and surround flow catheter irrigation: impedance-based appraisal in clinical ablation. *JACC Clin Electrophysiol*. 2017;3:1080-1088.
10. Kawaji T, Hojo S, Kushiyama A, et al. Limitations of lesion quality estimated by ablation index: an in Vitro Study. *J Cardiovasc Electrophysiol*. 2019;30:926-933.
11. Pérez FJ, Schubert CM, Parvez B, Pathak V, Ellenbogen K, Wood MA. Long-term outcomes after catheter ablation of cavo-tricuspid isthmus dependent atrial flutter: a meta-analysis. *Circ Arrhythm Electrophysiol*. 2009;2:393-401.
12. Brugada J, Katritsis DG, Arbelo E, et al. ESC Scientific Document Group 2019 ESC guidelines for the management of patients with supraventricular tachycardia. *Eur Heart J*. 2019;41(5):655-720.
13. Klimek-Piotrowska W, Hołda MK, Koziej M, et al. Clinical anatomy of the cavotricuspid isthmus and terminal crest. *PLoS ONE*. 2016;11:e0163383.
14. García-Dora J, Pérez-Rodon J, Rodriguez-García J, et al. Predictors of acute inefficacy and the radiofrequency energy time required for cavotricuspid isthmus-dependent atrial flutter ablation. *J Interventional Cardiac Electrophysiol*. 2017;49:83-91.
15. Paetsch I, Sommer P, Jahnke C, et al. Clinical workflow and applicability of electrophysiological cardiovascular magnetic resonance-guided radiofrequency ablation of isthmus-dependent atrial flutter. *Euro Heart J Cardiovasc Imaging*. 2019;20:147-156.
16. Kumar S, Morton JB, Lee G, Halloran K, Kistler PM, Kalman JM. High incidence of low catheter-tissue contact force at the cavotricuspid isthmus during catheter ablation of atrial flutter: implications for achieving isthmus block. *J Cardiovasc Electrophysiol*. 2015;26:826-831.
17. Baccillieri MS, Rizzo S, De Gaspari M, et al. Anatomy of the cavotricuspid isthmus for radiofrequency ablation in typical atrial flutter. *Heart Rhythm*. 2019;16:1611-1618.
18. Maclean E, Simon R, Dhillon G, Ahsan S, Hunter RJ, Behar JM. Use of ablation index to understand lesion delivery in the era of contact force guided ablation for cavo-tricuspid isthmus dependent atrial flutter. *Euro J Arrhythmia Electrophysiol*. 2019;5.
19. Reichlin T, Lane C, Nagashima K, et al. Feasibility, efficacy and safety of radiofrequency ablation of atrial fibrillation guided by monitoring of the initial impedance decrease as a surrogate of catheter contact. *J Cardiovasc Electrophysiol*. 2015;26:390-396.
20. Shah D, Lambert H, Nakagawa H, Langenkamp A, Aeby N, Leo G. Area under the real-time contact force curve (force-time integral) predicts radiofrequency lesion size in an in Vitro Contractile Model. *J Cardiovasc Electrophysiol*. 2010;21:1038-1043.
21. Zhang T, Wang Y, Han Z, et al. Cavotricuspid isthmus ablation using ablation index in typical right atrial flutter. *J Cardiovasc Electrophysiol*. 2019;30:2414-2419.

How to cite this article: Maclean E, Simon R, Ang R, et al. A multi-centre experience of ablation index for evaluating lesion delivery in typical atrial flutter. *Pacing Clin Electrophysiol*. 2021;1-8. https://doi.org/10.1111/pace.14228